

Fermi National Accelerator Laboratory

FERMILAB-Conf-93/388-E

DØ

A Search for Rapidity Gaps in Jet Events and a Study of Color Coherence in Multijet Events at DØ

Fred Borcharding
for the DØ Collaboration

*Fermi National Accelerator Laboratory
P.O. Box 500, Batavia, Illinois 60510*

December 1993

Presented at the *9th Topical Workshop on Proton-Antiproton Collider Physics*,
Tsukuba, Japan, October 18-22, 1993

Disclaimer

This report was prepared as an account of work sponsored by an agency of the United States Government. Neither the United States Government nor any agency thereof, nor any of their employees, makes any warranty, express or implied, or assumes any legal liability or responsibility for the accuracy, completeness, or usefulness of any information, apparatus, product, or process disclosed, or represents that its use would not infringe privately owned rights. Reference herein to any specific commercial product, process, or service by trade name, trademark, manufacturer, or otherwise, does not necessarily constitute or imply its endorsement, recommendation, or favoring by the United States Government or any agency thereof. The views and opinions of authors expressed herein do not necessarily state or reflect those of the United States Government or any agency thereof.

A Search for Rapidity Gaps in Jet Events and a Study of Color Coherence in Multijet Events at D0

Fred Borcharding
D0 Department/Research Division
Fermilab, Batavia, Illinois, US.
 for the D0 Collaboration

We present studies of Rapidity Gaps and Color Coherence in jet events at the D0 Detector for data taken during the recent Tevatron collider run at $\sqrt{s} = 1.8$ TeV. An upper limit of $f(\Delta\eta_C > 3) < 1.2 \times 10^{-2}$ @ 95% C.L. on the true rapidity gap fraction is given. The color coherence results indicate the angle ordering approximation as modeled in the Herwig monte carlo represents the collider data well.

1. Introduction

This paper presents some of the results of two separate analyses of data taken by the D0 Detector Collaboration during the recent '92-93 Tevatron Collider run at $\sqrt{s} = 1.8$ TeV. A study of Rapidity Gaps in jet events is presented first [1]. Then a study of Color Coherence in multijet events is presented.

2. What is a Rapidity Gap?

A rapidity gap is defined as a region of pseudo-rapidity with no particles in the final state. How this might look on a particle lego plot it is illustrated in figure 1. The rapidity gap region, unshaded, is a rapidity interval in which there are no particles.

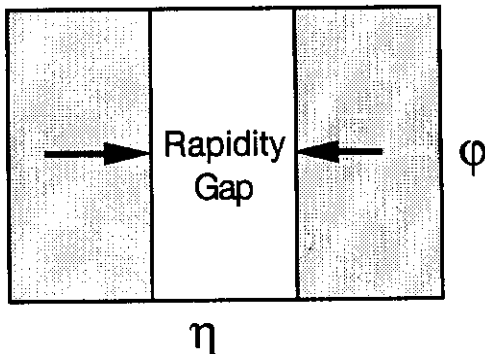


Figure 1: Rapidity gap on a particle Lego plot.

Rapidity gaps are expected to occur between jets in a color singlet exchange. (See figure 2.) In a color singlet exchange there are no color lines between the two hard scattered partons.

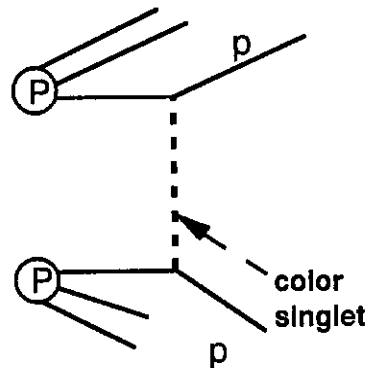


Figure 2: Color singlet exchange in collider event.

Since there are no color lines, destructive interference for radiation between the two

hard scattered partons will result in no particles in the rapidity interval.

On a jet lego plot this might look like figure 3. There are two leading jets from the hard scattered partons and the rapidity interval between the two jets contains no particles.

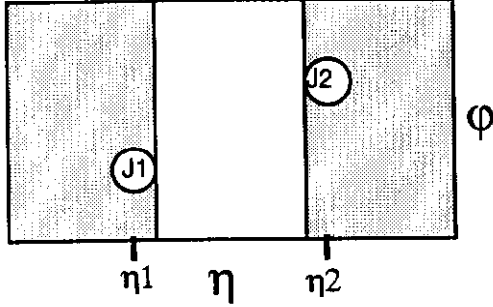


Figure 3: The rapidity interval in η vs. ϕ space.

The rapidity interval is

$$\Delta\eta_c = |\eta_1 - \eta_2| - 2R \quad (1)$$

where R is the jet cone radius. The rapidity interval is defined as the rapidity range between the inside edges of the two leading jets.

The rapidity gap fraction is

$$f(\Delta\eta_c) = \frac{\sigma_{\text{gap}}(\Delta\eta_c) \langle |S|^2 \rangle}{\sigma(\Delta\eta_c)} \quad (2)$$

Where $\sigma_{\text{gap}}(\Delta\eta_c)$ is the cross section for producing no particles between the leading 2 jets separated by the given rapidity interval, $\sigma(\Delta\eta_c)$ is the inclusive cross section for two leading jets with a given rapidity interval, and $\langle |S|^2 \rangle$ is the survival probability of the gap for a given rapidity interval. The survival probability means that there is no spectator interaction in a rapidity gap event. Estimates of the survival probability range from 10% to 30% [2,3,4].

The total rapidity gap cross section is

$$\sigma_{\text{gap}}(\Delta\eta_c) = \sigma_{\text{gap}}^{\text{singlet}}(\Delta\eta_c) + \sigma_{\text{gap}}^{\text{octet}}(\Delta\eta_c) \quad (3)$$

for a given rapidity interval size and is the sum of a color singlet plus a color octet term.

The color octet term involves color exchange between the leading jets. Therefore the number of jets in the rapidity interval is expected to follow the binomial distribution. The probability that this distribution fluctuates to zero will fall rapidly as the interval between the two leading jets increases. It is predicted [2] that the color octet rapidity gap cross section could fall as a simple exponential. However, this has not been tested for large rapidity intervals.

Since the color singlet term involves no color exchange it is expected that the cross section will not depend strongly on the rapidity interval size. Under certain simple assumptions the cross section could be constant with interval size [2]. A calculation for color singlet QCD exchange using a Pomeron model where the Pomeron is modeled as a pair of gluons was made [2]. For this model it was determined that the ratio of the color singlet cross section to the total dijet cross section could be as large as 10^{-1} . Another calculation where the color singlet exchange is electroweak [3] such as a γ , W or Z exchange, determined that the ratio should be in the range of 10^{-3} .

Combining the expected range of ratios with the smaller value, 10%, of the survival probability it is expected that the rapidity fraction will be in the range

$$10^{-2} > f(\Delta\eta_c > 3) > 10^{-4} \quad (4)$$

3. Data Sample and Cuts

In an ideal detector the rapidity gap fraction could be defined as

$$f(\Delta\eta_c)^{\text{true}} = \frac{N_{n=0}(\Delta\eta_c)}{N(\Delta\eta_c)} \quad (5)$$

where $N_{n=0}$ is the subset of events for a given rapidity interval with no particles between the leading jets. This true rapidity gap fraction cannot be measured in an actual detector. Tracking chambers only see

charged particles so neutral particles are missed. Calorimeters see energy flow not particles, they have efficiencies of less than 100%, and they also have some minimum threshold on the energy level they are sensitive to.

The full tracking information was not yet available so this study was done looking at the energy deposited in the calorimeter electromagnetic, EM, towers [5]. An EM tower subtends 0.1×0.1 in η vs. ϕ . The measured rapidity gap fraction was defined as

$$f(\Delta\eta_c)^{\text{measured}} = \frac{N_{\#EM=0}(\Delta\eta_c)}{N(\Delta\eta_c)} \quad (6)$$

where $N_{\#EM=0}(\Delta\eta_c)$ is the subset of events with no EM towers with energy > 200 MeV for a given rapidity interval.

Efficiency to deposit 200 MeV in EM

Particle	2 GeV	5 GeV
e/π^0	96%	>99%
π^\pm	40%	60%

Table 1 The efficiency for detecting 200 MeV of energy in an EM calorimeter tower for particles of different incident energy.

The average energy deposited by a minimum ionizing particle in an EM tower is 200 MeV. Table 1 gives the efficiencies for low energy particles as measured in a test beam [10].

The data was taken with two triggers, both of which used the calorimeter trigger which was instrumented out to $|\eta| \leq 3.2$. The first trigger was the standard trigger used for the inclusive jet cross section and was prescaled throughout most of the run. The second trigger, the high rapidity interval trigger, was a special trigger for this analysis. This high interval trigger was run un-prescaled and added significant statistics to the data sample for rapidity intervals greater than 2.6. At the hardware level this trigger required two jets each with $|\eta| > 2$, and at the software level the rapidity interval was required to be $\Delta\eta_c > 2.6$. Note that this trigger required a rapidity interval only and made no requirement on what was in the interval.

In the off-line analysis the inclusive trigger was used for the events with a rapidity interval less than 2.6 and the high interval trigger was used for the events with a rapidity interval greater than 2.6. Events with multiple interactions were removed since the presence of a second interaction could mask a rapidity gap event. The timing distribution for the level 0 scintillator hodoscopes was used to determine if a crossing had more than one interaction. The level 0 hodoscope information alone was 75% efficient for finding a single interaction event and less than 5% of the time identified a multiple interaction event as a single interaction [6]. The D0 standard jet algorithm was used with a jet cone size of 0.7 [7]. The D0 standard jet cuts were also made to remove hot cells and main ring background. This cut was about 95% efficient in removing backgrounds and removed about 4% of real jets [8]. The D0 standard jet energy scale correction was also made to all jets before cuts. This energy correction increased the energy of each jet by an average of 15% [9]. The interaction vertex was required to

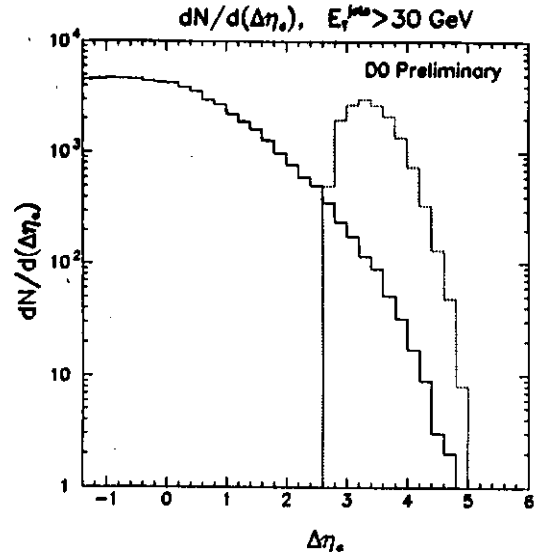


Figure 4: Distribution of the number of triggers. The solid line is the inclusive trigger, the dotted line is the high rapidity interval trigger

be within 50 cm of the detector center. The rapidity interval was required to be greater than 0. The transverse energy of each of the

two leading jets was required to be greater than 30 GeV. Also the η boost was required to be, $|\ln(\text{boost})| = |1/2(\eta_1 + \eta_2)| < 0.8$ to keep the rapidity interval centered on the Central EM Calorimeter which had a higher efficiency.

After these offline cuts the data sample consisted of 27.5K events from the inclusive trigger and 15.4K events from the high interval trigger. Figure 4 shows the number of events for each value of the rapidity interval. From the figure it is seen that the high interval trigger adds significant statistics for interval values > 2.6 . Also there are events out to a rapidity interval of 5.

Isolated calorimeter cells, that is cells not in jets, occasionally have false energy. These noisy cells were caused by high voltage discharge, electronics noise or uranium noise. These cells if left in the data would artificially suppress the rapidity gap fraction. The noisy cells were removed by suppressing any EM towers which had a cell in them with an occupancy of $> 3\sigma$ over the average occupancy for all the cells in the same η ring. This average was taken over the entire data set and reduced the acceptance by $< 0.5\%$.

4. Results

Figure 5 shows preliminary results for the measured gap fraction defined in equation 6. The vertical axis is the measured rapidity gap fraction plotted on a log scale. The horizontal axis is the rapidity interval and ranges from 0 to 5. The transverse energy of each of the two leading jets is required to be > 30 GeV. The error bars shown are statistical errors only.

The behavior at $\eta < 2$ is suggestive of the naive expectation for the color octet contribution. The measured fraction falls rapidly on a log plot from a value of 1 at an interval size of 0. The behavior for $\eta > 3$ is suggestive of the naive expectation for the color singlet contribution since the measured gap fraction seems to level off, approaching a constant value. At this time, however, it is premature to reach these conclusions. The leveling off at large rapidity interval could be due to

inefficiencies in the EM calorimeter. For example detector inefficiencies would miss particles in the interval and enhance the measured gap signal. Alternatively the deviation from steep fall off could be due to structure in the color octet contribution. At larger rapidity intervals the color octet contribution could differ significantly from simple exponential fall off since this color octet contribution has not been measured before.

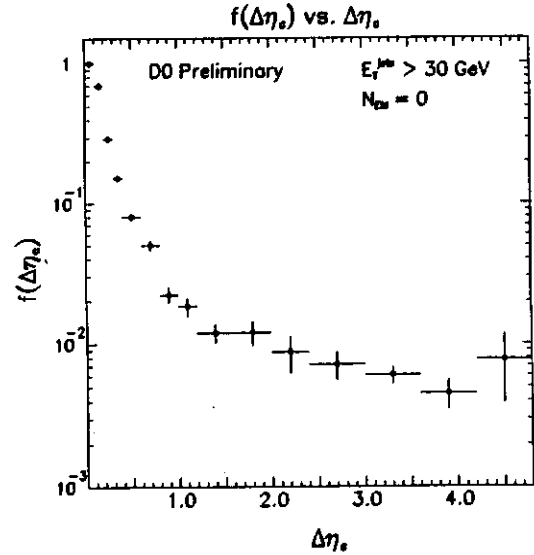


Figure 5: Preliminary results for the measured rapidity fraction.

The measured rapidity gap fraction is

$$f(\Delta\eta_c > 3) = 5.7 \pm 0.7 \pm 0.6 \times 10^{-3} \quad (7)$$

for the data at rapidity interval > 3 . The 0.7 is the statistical error and 0.6 is the systematic error. The systematic error consists of a 7% error from the jet energy scale correction, a 5% error from the noisy cells correction, a 5% error from the single interaction correction, and a 5% error from the standard jet cut correction.

5. Upper Limit on True Rapidity Gap Fraction

To determine the true rapidity gap fraction from the measured, corrections would have to be determined for all the effects which could make the measured value

differ from the true value. The most obvious of these effects is detector inefficiencies. Due to detector inefficiencies a real deposit of energy above threshold in an EM tower could be measured at less than the cut value giving a fake gap event. If we set an upper limit on the true gap fraction then, to first order, we need only make corrections for those effects which would make the measured gap fraction less than the true gap fraction.

There are two effects which make the measured rapidity gap fraction less than the true fraction, out-of-cone fragmentation and shower broadening. Out-of-cone fragmentation occurs when the original hard scattered parton fragments into particles one or more of which fall outside of the 0.7 cone size. Shower broadening

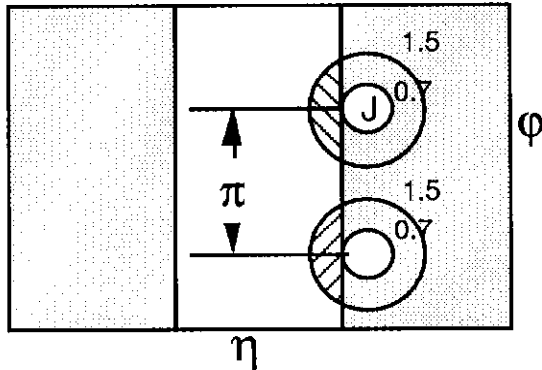


Figure 6: Definition of area for out-of-cone correction.

occurs when the shower from the jet particle(s) fluctuates transversely outside the 0.7 cone size. In the EM calorimeter these two effects are indistinguishable and both effects could deposit energy in the rapidity interval of true rapidity gap events.

A study was made to determine the correction for these effects using all the leading jets in events with a rapidity interval > 3 . A cone of radius 1.5 was drawn around each of the jet cones of radius 0.7 forming an annulus around each of the jets. The area of overlap of this annulus with the rapidity interval was taken, this is the cross-hatched area in figure 6. In this area the number of towers above threshold measures the number from out-of-cone

plus the number from the underlying event. Next a similarly defined area at $\phi = 180^\circ$ from the leading jet was taken. In this area the number of towers measures the number from underlying events. The number of EM towers around the leading jet minus the number of EM towers from the away area equals the number of EM towers around the leading jet from out-of-cone and shower broadening effects. The study indicated that 40% of the events are contaminated by out-of-cone and shower broadening.

Folding in this correction a preliminary upper limit on the true rapidity gap fraction for rapidity intervals > 3 is

$$f(\Delta\eta_C > 3)^{\text{true}} < 1.2 \times 10^{-2} \quad \text{@ 95\% C.L.} \quad (8)$$

This value is at the upper boundary of the naive estimates given earlier.

6. Rapidity Gap Conclusions

In conclusion D0 does see events with a rapidity gap when that gap is defined as in equation 6, the measured gap fraction was given in equation 7, and an upper limit on the true rapidity gap fraction was given in equation 8. This limit is independent of the experimental definition and gives the upper limit on particles in the rapidity interval.

Future plans include adding the remaining parts of the calorimeter, including the inter-cryostat detector, the massless gaps and the hadron calorimeter, to fill in the holes of the EM calorimeter. Future plans also include expanding the analysis to include tracks in the central and forward drift chambers.

7. Color Coherence

R. K. Ellis et al. in reference 11 present a method of calculating the probability for the emission of a soft gluon in a hard process, $2 \rightarrow 2 + \text{soft parton}$, inside a soft gluon cone. The soft gluon emission cone (see figure 7) around parton 2 has as its cone axis the parton 2 direction and as its cone angle the angle between parton 2 and the closest other parton, in this case the beam parton (+). They continue by defining

the angle ordering approximation as the approximation that soft gluons are only emitted in the soft radiation cones. Then

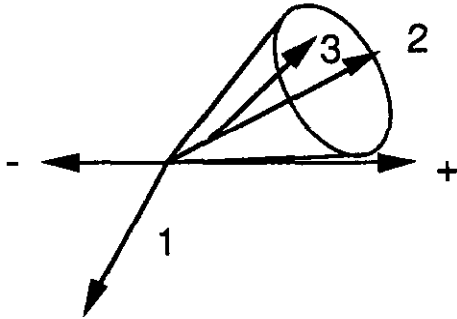


Figure 7: Soft gluon emission cone.

soft parton 3 can only be emitted at $\theta_{32} < \theta_{2+}$, the angle of jet 2 with respect to the nearest beam jet.

What this might look like on a jet lego plot is illustrated in figure 8, when the transverse energy of the jets is ordered such that $ET_1 > ET_2 > ET_3$. Jets 1 and 2 are from the hard scattered partons and the cross hatched area labeled 3 is the soft radiation cone around jet 2.

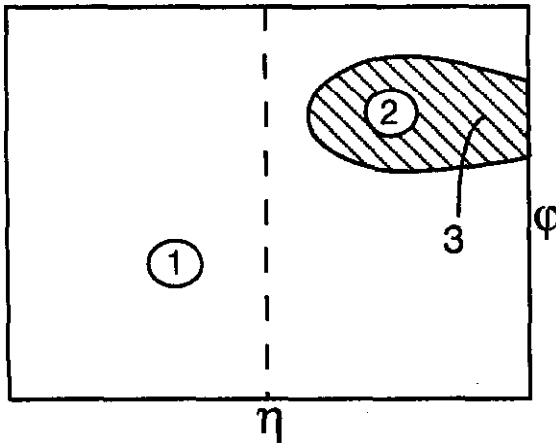


Figure 8: Soft gluon emission area in η vs. ϕ .

From this plot we see that one would expect more soft jets to be produced at the same ϕ as jet 2 both forward and backward in η , than at the same η but different ϕ .

8. Data Sample

The analysis at D0 used data taken during the '92-93 run using the Jet_High trigger. This trigger required one jet in the

hardware trigger with transverse energy greater than 80 GeV and a cone size of 0.7 and was active for the entire 15pb^{-1} exposure.

The off-line analysis used the D0 standard jet cut which removed main ring background and hot cells. Three or more jets were required in the events. The leading jet transverse energy was required to be greater than 100 GeV to ensure the efficiency of the trigger. The transverse energy of the third jet was required to be

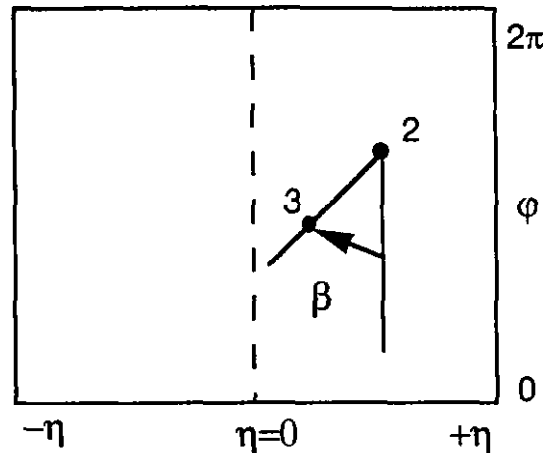


Figure 9: Definition of the β variable.

greater than 10 GeV to ensure the efficiency of the jet finding algorithm. Also the two leading jets were required to be back to back in ϕ to within 20° to enrich the sample with soft gluon jets.

Monte Carlo data was also generated using the Herwig MC which includes angle ordering, and the Isajet MC which does not. The MC events were processed through a Geant detector simulation and subjected to the same analysis as the collider data.

The results were looked at in β plots for various values of the jet cone size, different rapidity ranges for the two leading jet η 's, and for different R disks. R is the distance in η/ϕ space and an R disk is the area of an annulus between a minimum and maximum radius R. The definition of β as shown in figure 9 is the angle of the soft jet relative to the 2nd jet. When $\beta = \pi/2$ the soft jet is between the 2nd jet and the far beam jet and when $\beta = 3\pi/2$ the soft jet is between the 2nd jet and the near beam jet.

9. Color Coherence Results

Preliminary results are presented for both collider and monte carlo data using a jet cone size of 0.5, where both $|\eta_1|$ and $|\eta_2|$ are restricted to be less than 0.7, and the R disk is limited to the region, $0.8 < R < \pi$. These values were chosen because they

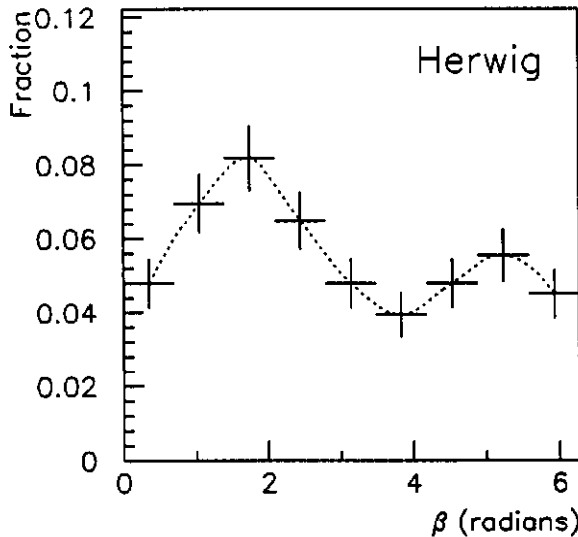


Figure 10a: Plot of β for Herwig MC generated events.

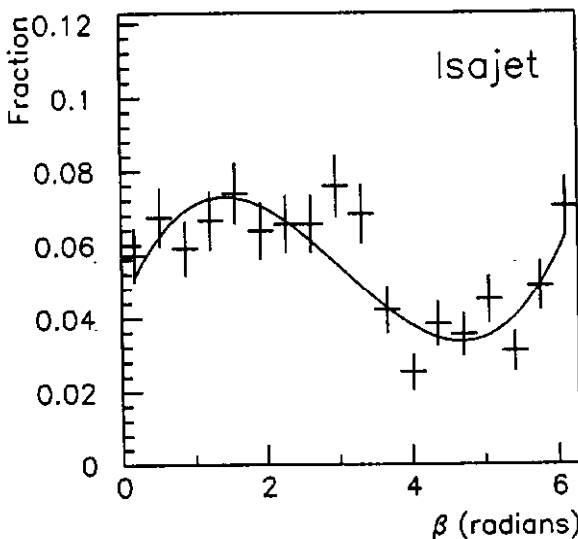


Figure 10b: Plot of β for Isajet MC generated events.

clearly show a difference between the

Herwig and Isajet results, and these values of parameter space pass a large statistics sample of the data.

Figure 10a shows the β for Herwig MC generated jet events. The vertical axis is the fraction of events of the total number of events in a particular β bin. The error bars are the statistical error on the MC data. The dotted line is a smooth curve drawn

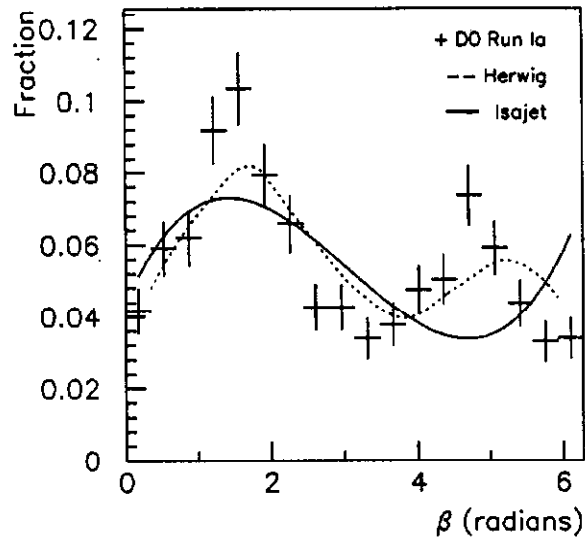


Figure 10c: Plot of β for collider data. The curves are from Herwig and Isajet MC.

through the MC points. Figure 10b shows a similar plot for the Isajet MC events with the error bars representing the statistical errors. The solid line is a 3rd order polynomial fit to the MC data and is meant to be representative only of the MC data, not a rigorous fit since such a fit would require the fit function to be periodic with period 2π . The most noticeable difference between these two plots is the peak at $3\pi/2$ seen in the Herwig data with a contrasting valley seen in the Isajet data. Figure 10c shows the preliminary data from collider events with only statistical errors shown. The solid and dotted lines are the Isajet and Herwig curves respectively from the earlier plots. The collider data seems to have a pronounced peak at $3\pi/2$ which agrees well with the Herwig values, but not

at all well with the Isajet values.

10. Color Coherence Conclusion

In conclusion preliminary results from D0 collider data for jets seem to confirm the

existence of angle ordering as modeled by the Herwig monte carlo. In the future work is planned to increase the statistics of the MC samples and to pursue a systematic study of the data and MC through more of the available parameter space.

References

- [1] S. Abachi et al. (D0 Collaboration), "A Search for Jet Events with Rapidity Gaps in pp collisions at $\sqrt{s} = 1.8$ TeV", Submitted to Phys. Rev. Lett.
- [2] J. D. Bjorken, Phys. Rev. **D47** (1992) 101.
- [3] H. Chehime et al., Phys. Lett. **B286** (1992) 397.
- [4] E. Gotsman, E. M. Levin and U. Maor, Phys. Lett. **B309** (1993) 199.
- [5] S. Abachi et al. (D0 Collaboration), "The DZero Detector", submitted to Nucl. Instr. and Methods in Phys. Research A, FERMILAB-PUB-93/179.
- [6] J. Bantly, "Multiple Interaction Tool Study", D0 Note 1849 (1993) (unpublished).
- [7] N. Hadley, "CAHITS and CAJETS packages for Calorimeter Analysis", D0 Note 1006 (1990) (unpublished).
- [8] D. Elvira, "Study of Standard Jet Cuts and their Efficiencies Using D0 Collider Data", D0 Note 1763 (1993) (unpublished).
- [9] A. Milder and R. Astur, "Jet Energy Calibration Using the Missing ET Projection Fraction", D0 Note 1657 (1993) (unpublished); A. Milder and R. Astur, "Jet Energy Scale Corrections", D0 Note in progress (1993) (unpublished).
- [10] J. Kotcher, Ph.D. Thesis submitted to New York University (1992).
- [11] R. K. Ellis et al., "Soft Radiation in Parton-Parton Scattering", Nucl. Phys. **B286** (1987) 643.